FLUX FLOW AND FLUX DYNAMICS IN HIGH-T_C SUPERCONDUCTORS

L.H. Bennett, M. Turchinskaya, L.J. Swartzendruber, A. Roitburd, D. Lundy, J. Ritter, and D.L. Kaiser

Materials Science and Engineering Laboratory
National Institute of Standards and Technology
Gaithersburg, MD 20899

Many of the potential applications of the high-temperature superconductors require a pinning mechanism for flux lattice stabilization in the mixed state in order to provide high critical currents and high levitation forces. Three aspects of flux pinning are reviewed here:

(i) The magnetic properties of single crystals of YBCO, including such topics as anisotropy in the flux pinning and in the critical current density, and the effects of twins on the flux pinning and on the lower critical field.

(ii) A critical field for depinning, H_{cp}, can be defined as that field at which the hysteresis loop changes from irreversible to reversible. Measuring BSSCO as a function of temperature, H_{cp} can be described by a power law with an exponent of 1.5.

(iii) When the applied field is changed rapidly, the time dependence of flux change can be divided into three regions, an initial region which occurs very rapidly, a second region in which the magnetization has a ln(t) behavior, and a saturation region at very long times.

INTRODUCTION

When a magnetic field, H, is applied to a type II superconductor which has been cooled below its critical temperature in zero magnetic field, all magnetic flux is excluded from the specimen for $H<H_{c1}$, where H_{c1} is the lower critical field. For $H>H_{c1}$, magnetic flux penetrates the specimen, and a vortex state of mixed normal and superconducting regions exists up to the upper critical field, H_{c2} [1]. In this mixed state, superconducting currents circulate in planes perpendicular to the magnetic flux lines and form vortices threading the specimen. These vortices can be anchored by defects in the material called pinning centers. This pinning inhibits movement of vortices into or out of the specimen. Thermal activation of the vortices over the pinning centers results in flux creep. The flux gradient that occurs due to the presence of pinning forces gives rise to hysteresis in the magnetization vs applied field curve. At any given applied field, the width of this hysteresis loop is proportional to the "magnetic critical current", J_c. At high fields (but still with $H<H_{c2}$), the forces on the vortices can exceed the pinning forces. The width of the hysteresis loop then shrinks to zero and J_c vanishes, and in the sense that transport current will not flow without resistance, the material is no longer "superconducting". Finally, for $H>H_{c2}$, the density of vortices becomes so large that the individual vortices overlap, resulting in complete penetration of the field and a loss of superconductivity.

Because high-temperature superconductors, including $YBa_2Cu_3O_{6+x}$ (YBCO) and Bi-Sr-Ca-Cu-O (BSCCO), are type II superconductors with relatively low H_{c1} values and high H_{c2} values, they will be in a "critical state" for many of their applications. In the critical state, with the effective field between H_{c1} and H_{c2}, flux lines have penetrated the material and are pinned by structural defects, chemical inhomogeneities, and impurities. A detailed knowledge of how flux penetrates the materials and its behavior under the influence of applied fields and current flow, and the effect of material processing on these properties, is required in order to apply, and to improve, the properties of these superconductors.

SINGLE CRYSTAL YBCO

YBCO single crystals have been grown from the melt using a technique described by Kaiser *et al.* [2]. The plate-like morphology of some of these crystals can be seen in Figure 1. Magnetization studies have established that flux pinning in YBCO single crystals is highly anisotropic [3-8]. When a magnetic field is applied parallel to the c-axis, the flux lines are strongly pinned, contributing to high critical currents within the Cu-O planes. In contrast, weak pinning between the Cu-O planes contributes to low critical currents for applied fields perpendicular to the c-axis. This difference in pinning manifests itself in a large anisotropy in the hysteresis loops when a magnetic field is applied parallel to and perpendicular to the c-axis of the crystal, as is evident in Figure 2 [9]. These loops were measured on a nearly cubic single crystal (120x135x120 μm^3). The cubic morphology of the crystal has allowed a clear determination of the anisotropy of the critical current density without the complication of large, and differing, demagnetization factors. Our measured anisotropy, (Jc//c)/(Jc $\perp$ c), is 62 at 10K in an applied field of 10 Oe, which is higher than that reported previously for comparable conditions.

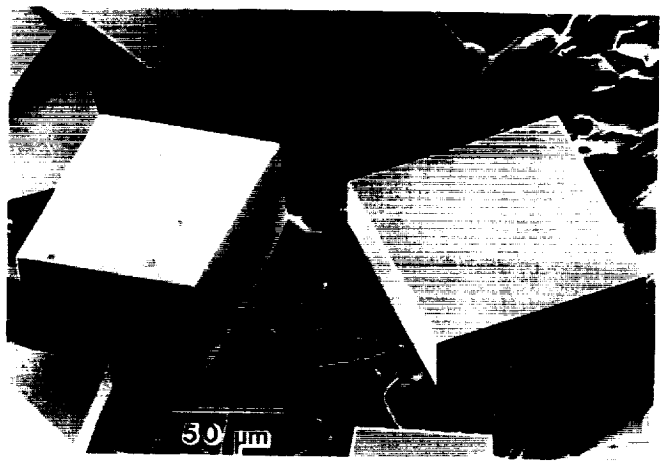

Figure 1. Scanning electron micrograph of some single crystals of YBCO grown from the melt [2].

The observed anisotropy in flux pinning suggests directionality in the distribution or strength of pinning centers. One proposed anisotropic pinning center in single crystals is twin boundaries [4,10] which form in the material during cooling through the tetragonal to orthorhombic transition. The (110) and ($1\bar{1}0$) twin planes lie parallel to the c-axis, with typical spacing between planes of 20 to 2000 nm [2]. A difference in the interaction energy of flux lines and twin boundaries would be expected for flux lines threading through the crystal parallel and perpendicular to the twin planes.

Several high-resolution Bitter-pattern studies [11, 12] have shown that twin boundaries

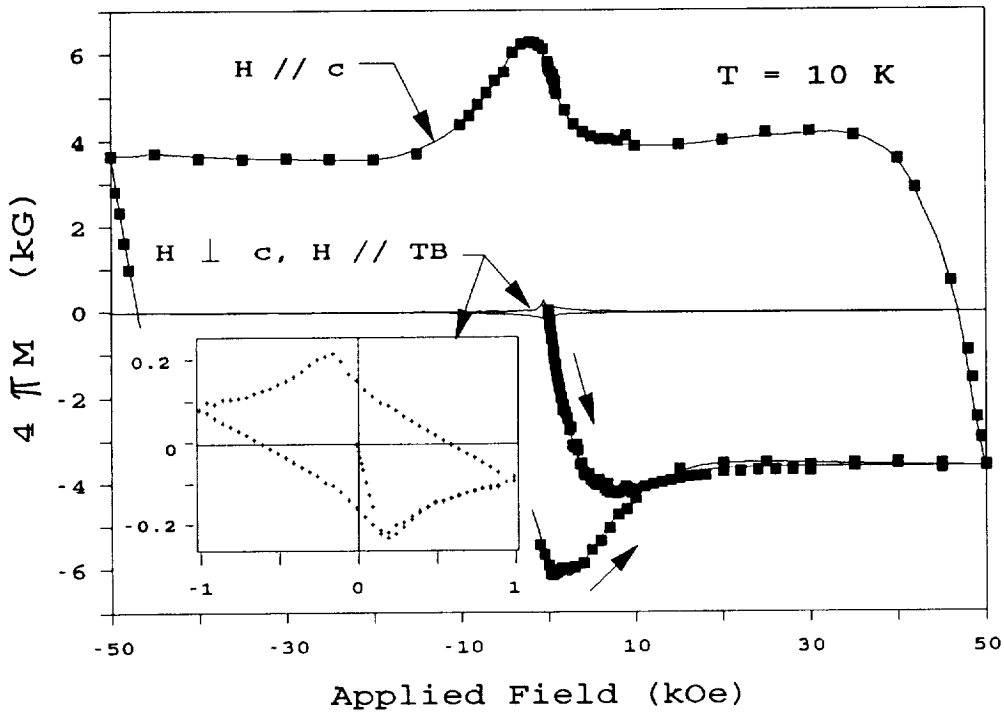

Figure 2. Hysteresis loops at 10K for a YBCO single crystal for fields applied parallel to and perpendicular to the c-axis. The large difference in the widths of the two loops is due to anisotropy of the critical current.

do indeed pin flux lines, resulting in vortex lattices which are clearly correlated with the twin boundary orientation. However, well-developed vortex lattices have also been observed in twin-free regions [12], indicating that other intrinsic crystalline defects such as oxygen vacancies act as pinning centers. Gyorgy et al. [13] recently determined that there was not a significant difference between the critical current densities for flow within the Cu-O planes with an applied field parallel and perpendicular to the c-axis of a twinned crystal, leading them to conclude that twin boundaries are not the dominant pinning centers.

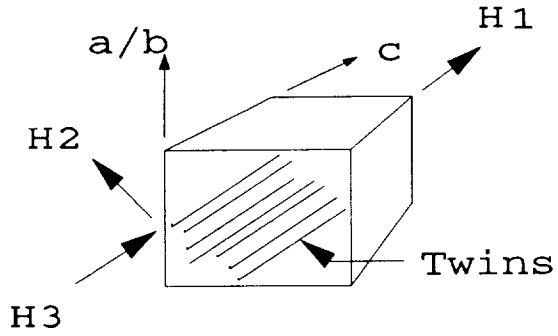

Figure 3. Geometry used to study the effect of twin boundaries on flux pinning. H1 is a field // to both the c axis and the twin boundaries; H2 is ⊥ to both c and the twins; H3 is ⊥ to c and // to the twins.

To study the effect of the twins on the flux pinning, the magnetic properties of the YBCO crystal whose hysteresis loops are shown in Figure 2 was investigated [9]. This crystal had predominantly one variant of twin boundary. Its geometry is sketched in Figure 3. Small differences in magnetic behavior were observed when the field was applied perpendicular to the c-axis and either parallel or perpendicular to the predominant twin boundary orientation, showing that twins have a direct measurable (but small) effect on flux pinning. An example is shown in Figure 4, where the shielding behavior of the crystal in the H1 direction (// to the c axis) is different than for the magnetic field ⊥ to the c axis, for either the H2 (⊥ to the twin planes) or

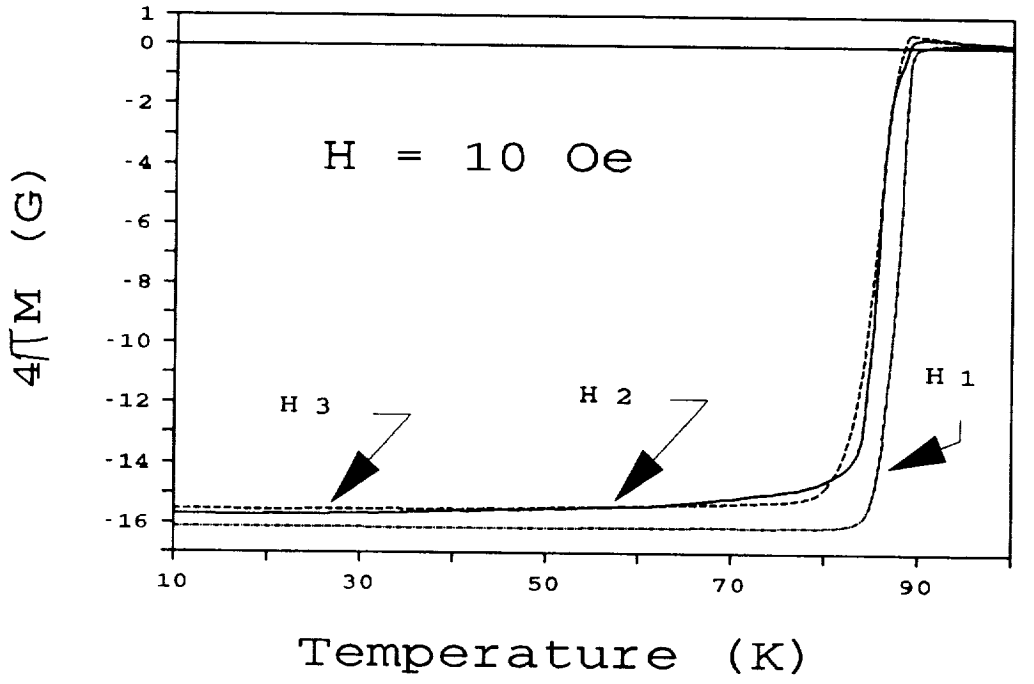

Figure 4. Shielding measurements for the same crystal taken upon heating in a field of 10 Oe, after cooling in zero field. H1, H2, and H3 are magnetic field directions defined in Figure 3.

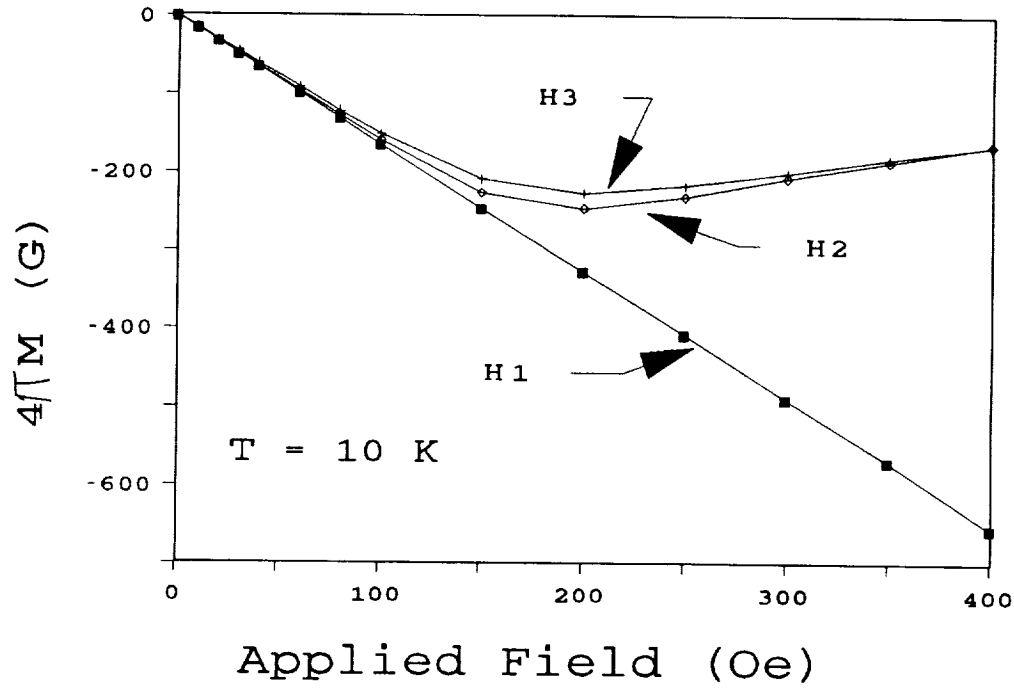

Figure 5. Magnetization curves after zero field cooling for the same crystal, with H1, H2, H3 as defined in Figure 3. H2 and H3 differ due to a difference in flux pinning for vortices ⊥ and // to the twin boundaries.

the H3 direction (// to the twin planes). A second example is shown in the magnetization curves depicted in Figure 5, where a magnetic field is applied to the zero-field-cooled sample for the three directions. Again the largest difference is due to crystalline anisotropy, whereas the behavior with respect to the twins is small, but real. The flux-vortex pinning is greater when the applied magnetic field is perpendicular to the twin boundaries at 10K. However this effect is temperature dependent and reverses at $\approx$80K [14], as is illustrated in Figure 6.

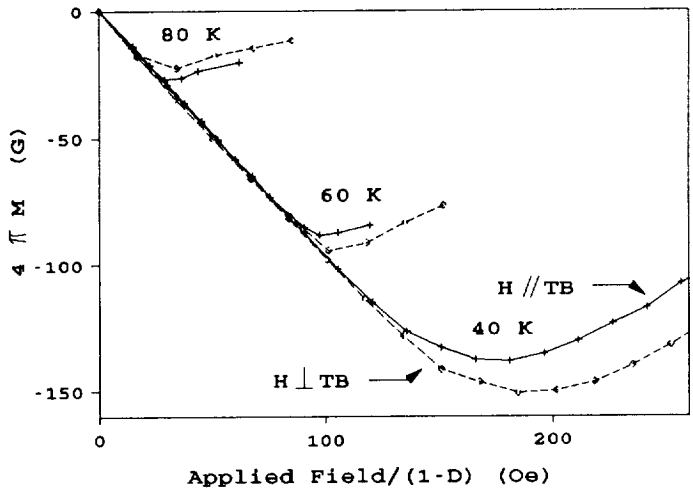

Figure 6. Magnetization vs applied field for two orientations of the same crystal. The applied field has been corrected for demagnetization (D=3).

The pinning mechanisms responsible for the high critical currents, J_c, seen in single crystals is of considerable interest. Although some of the highest J_c's for YBCO at 77K reported to date have been in single crystals, not all crystals have the same J_c. (We refer here to fully oxygenated single crystals, since J_c at 77K is lowered when the oxygen content is decreased enough to lower T_c below 90K.) A case in point is displayed in Figure 7, which shows a 77K hysteresis loop for a different YBCO single crystal than that shown in Figures 2-6. This crystal had dimensions of 200x178x75 μm^3, and has a higher T_c (93K) than the "cube" (T_c=89K) because of its lower concentration of impurities (trace amounts of Al, Si, Ca). The narrowness and characteristic shape of this loop shows that this crystal must have only a small amount of pinning. From this loop and the sample geometry with H//c, it can be estimated that this crystal has a magnetic J_c of $5x10^3 A/cm^2$ for H=0. This value is less than that reported for many single crystals and for quench and melt growth samples. It is larger than obtained in sintered samples (which show J_c's at 77K on the order of 100-1000A/cm^2)

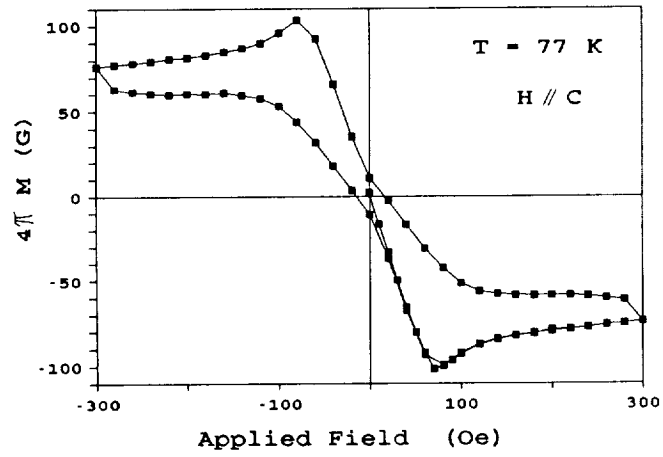

Figure 7. Hysteresis loop of a different single crystal of YBCO taken with the field applied parallel to the c axis.

Although no firm conclusions can be drawn at present, our experience indicates that the more perfect (geometry, purity, etc.)single crystals tend to have much lower J_c's, whether or not they contain twins. Further examples are given elsewhere in this conference, where the lower critical field was measured with high precision, and the temperature dependence of the Ginzburg-Landau parameter derived [15].

FLUX DEPINNING IN Bi SUPERCONDUCTORS

The occurrence of flux depinning, at a critical magnetic field which varies with temperature, has been observed in hysteresis loops of the high-T_C superconductors. The critical field for depinning is relatively low for the bismuth superconductors, with implications for both scientific understanding and technological applications. We report here on the results of magnetic measurements on a bismuth-based superconductor which displays three distinct phases.

The BSCCO superconducting oxides [16,17] have certain advantages over the 1-2-3 materials of which $YBa_2Cu_3O_7$ is the prototype. Among these advantages are a phase with a higher superconducting transition temperature (T_c), the lower cost of bismuth as compared to yttrium, ease of processing particularly with respect to annealing and in forming thin films, and indications of a higher stability with respect to air and moisture. Along with these advantages is the inherent disadvantage associated with the observed magnetic field dependence of their superconducting properties.

Many applications of the high T_C superconductors require the capability of carrying large currents. The critical current density arises from the equilibrium between the Lorentz force exerted by the transport current and the pinning forces operating on the magnetic flux lines. The flux lines often form a flux lattice so that a small number of pinning centers can pin many flux lines. The observation of a hysteresis loop conforming to the Bean critical-state model suggests the presence of strong flux pinning in $YBa_2Cu_3O_7$ [18]. In this model, the magnetic critical current is derivable from the loop parameters. In particular, the width of the hystresis loop at a given magnetic field can be used to calculate a critical current (generally referred to as the "magnetic critical current").

In conventional superconductors, the movement of flux lines occurs by flux "creep" when pinning is strong [19] and by flux "diffusion" when the transport current is large enough to overcome the pinning forces [20]. Both of these dissipative phenomena were observed [18] in the same sample of the high-T_C superconductor, $YBa_2Cu_3O_7$. In addition to these dynamic effects, a novel behavior is observed in the high T_C superconductors, namely a reversible-irreversible transition which was first found by Müller, Takashige, and Bednorz [21] during temperature sweeps in La_2CuO_{4-y}. At a given temperature, flux is depinned for fields higher than a critical field. A de Almeida-Thouless-like behavior was found to describe [22] the separation between reversible and irreversible behavior in the susceptibility. Similar flux depinning was also measured by a number of different kind of experiments in Y-Ba-Cu-O [23,24] and in Bi-Sr-Ca-Cu-O [24-28] high temperature superconductors.

One sample of a Bi-Pb-Sr-Ca-Cu-O high-T_C superconductor, with starting composition $Bi_{1.7}Pb_{0.25}Sb_{0.1}Ca_2Sr_2Cu_2O_x$, is particularly interesting in that it displays three distinct superconducting phases. The critical field for flux depinning found in this sample was low enough to permit its determination over a wide temperature range. We find that the temperature dependence of the critical field for flux depinning can be described by a 3/2 power law for all three phases.

The real and imaginary parts of the ac susceptibility were measured in a Hartshorn-type bridge with an applied ac field of about 40A/m (0.5Oe) at a frequency of 1.68kHz. The hysteresis loops were obtained in a vibrating sample magnetometer. The real part of the ac susceptibility reveals three distinct temperature ranges associated with three superconducting

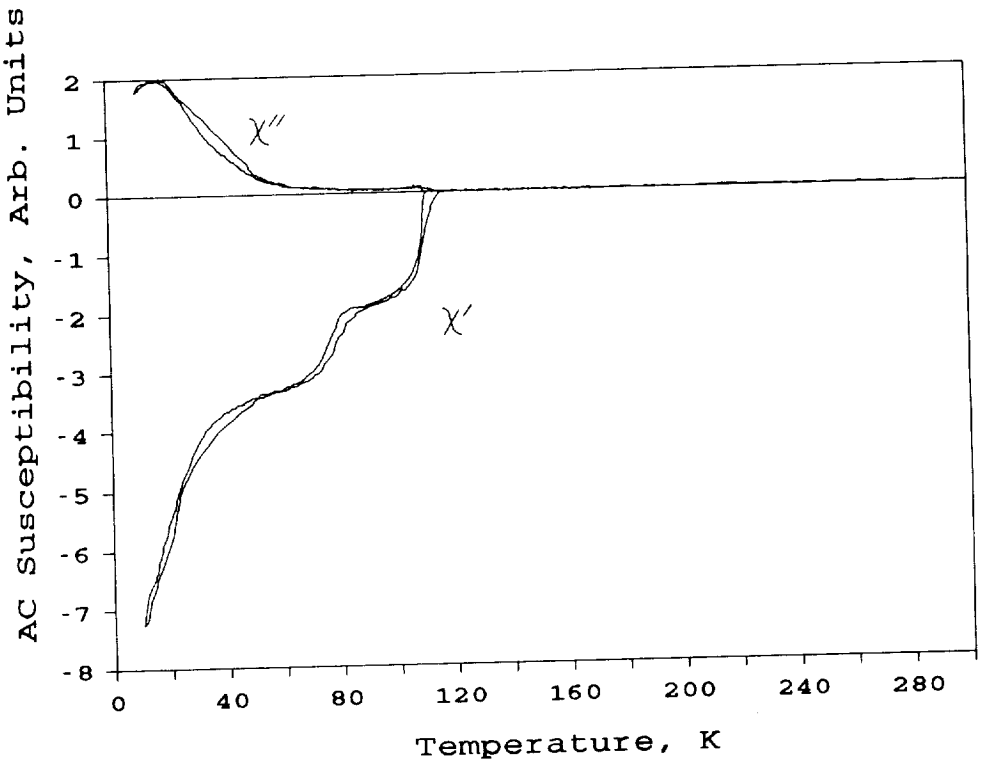

Figure 8. AC susceptibility of a Bi-oxide superconductor. The double traces are up and down temperature sweeps. The real part, χ', shows three distinct regions of superconductivity. The imaginary part, χ'', has less obvious peaks.

phases: (i) a fairly sharp diamagnetic transition starting above 110K, a second transition starting above 80K, and a third broad transition below 60K (see Figure 8). The imaginary part of the ac susceptibility shows a weak peak at about the center of the 10%/90% range of the 110K transition and a stronger peak associated with the 60K transition. These observations indicate that the sample was predominately three phase, but with a distribution of transition temperatures, most likely due to compositional variations within each phase.

Figure 9 shows a hysteresis loop at 105K for the same material used for the measurements in Figure 8. This loop is narrow, indicating the presence of only a small amount of flux pinning. In addition, the loop is constricted in the center, indicating the probable existence of dynamic effects similar to those found [18] in $YBa_2Cu_3O_7$. The hysteresis disappears in this loop for applied fields above $\approx$70Oe. This effect was observed previously (at somewhat different fields) in the hysteresis loops of Bi-Ca-Sr-Cu-O samples prepared by other techniques [27, 28].

Examination of the plots shown in Figures 9 and 10 suggests the existence of a critical depinning field, H_{cp}, above which flux pinning vanishes. The exact definition of such a critical field in our experiment has some uncertainty since the transition is gradual. We define the

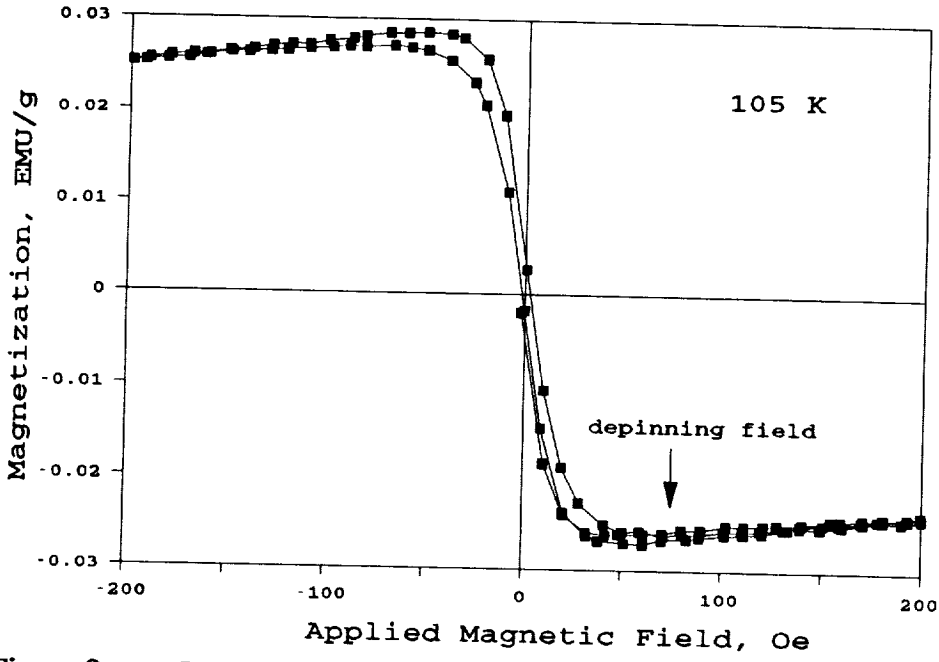

Figure 9. Hysteresis loop at 105K of the same Bi-oxide superconducting material as whose ac susceptibility is shown in Figure 1.

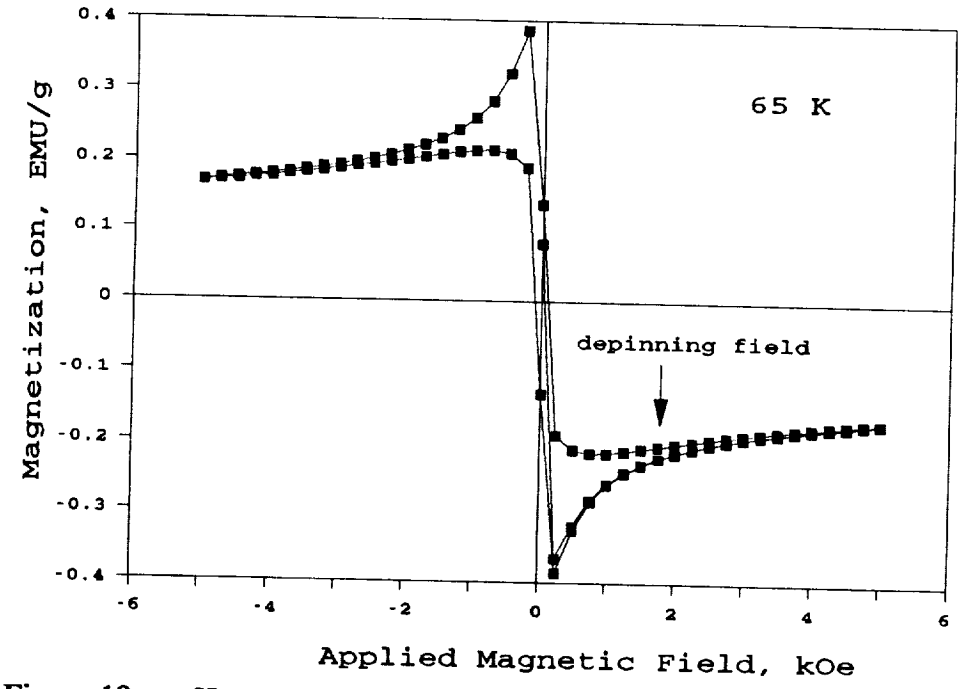

Figure 10. Hysteresis loop at 65K of the same Bi-oxide superconductor.

critical field, H_{cp}, as the field at which the separation between the magnetization for increasing and decreasing fields is less than one-twentieth the peak magnetization (see Figures 9 and 10). For a single phase sample (with a single value of T_c), a log-log plot of the critical field versus the temperature interval below the critical temperature should be a straight line, i.e.,

$$H_{cp}=H_{cp_o}(1-T/T_c)^n \qquad (1)$$

where the prefactor H_{cpo}, the value of H_{cp} at T=0, is a measure of the pinning strength for that superconducting phase. The appearance of a straight line when plotting $\ell(H_c)$ versus $\ell n(1-T/T_c)$ is very sensitive to the value of T_c chosen. The experimental data for our three-phase sample do not form a straight line, no matter what T_c is chosen.

We can, however, interpret the results as made up of three straight lines, the first obtained by plotting against $\ell(1-T/115)$, the second obtained by using $\ell(1-T/91)$, and the third using $\ell(1-T/52)$. An example is shown in Figure 11, for the data in the temperature range 35K to 85K. It is seen that the data between 50K and 80K fall on a straight line. All of the observed data, and the three fits, are displayed in Figure 12. Note that the straight line of Figure 11 appears as a curved line in Figure 12, since the abscissa is different.

The three numbers, 115K, 91K, and 52K, were chosen to give the three best linear fits for which the slope (exponent) is 1.5. When these temperatures are overlayed on the real part of the ac susceptibility results of Figure 8, Figure 13 is obtained. It then appears to be reasonable to consider these numbers as the real "onset" temperatures for the three superconducting phases. They have somewhat higher values than what might have have been chosen directly from the data of Figure 8.

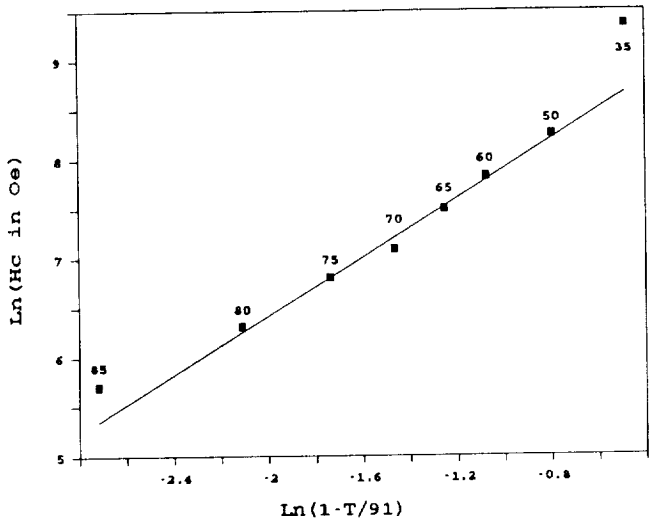

Figure 11. Log-log plot of critical field for flux depinning versus reduced temperature, assuming a critical temperature of 91K. The solid line is a linear fit for temperatures from 50 to 80K.

It is interesting to compare these results with earlier work [26] on magnetic measurements of the superconducting properties of a crystalline chunk, consisting of many small crystals, prepared by casting from the oxide melt with a starting composition of $Bi_3Ca_2Sr_2Cu_3O_x$. AC susceptibility revealed an onset temperature of 82 K and a transition width of $\approx$ 10 K. Hysteresis loops at 70 K showed a very small hysteresis, indicating a low density of effective flux pinning sites at this temperature, similar to the behavior observed for some superconducting samples of the Bi-Ca-Sr-Cu-O system prepared by other techniques. However, the magnetization at 10 K showed no hysteresis for fields greater than $\approx$3.5 kOe, a much smaller value than observed in the Bi sample reported on above. This critical field for

flux depinning, H_{cp}, appeared to vary with temperature as $H_{cp} = 4980(1-T/82)^{2.5}$. The exponent is very similar to what Lundy et al observed [27] in a different sample, but the prefactor is considerably different in the two samples. If, however, as discussed in [26], it is assumed that each sample consists of more than one phase, with more than one T_c, another interpretation of the data is posssible. Instead of fitting the data to one line, the H_{cp} values could be subdivided into several lines, each with a smaller slope than the average value. It thus appears that these data are also consistent with an exponent of 1.5.

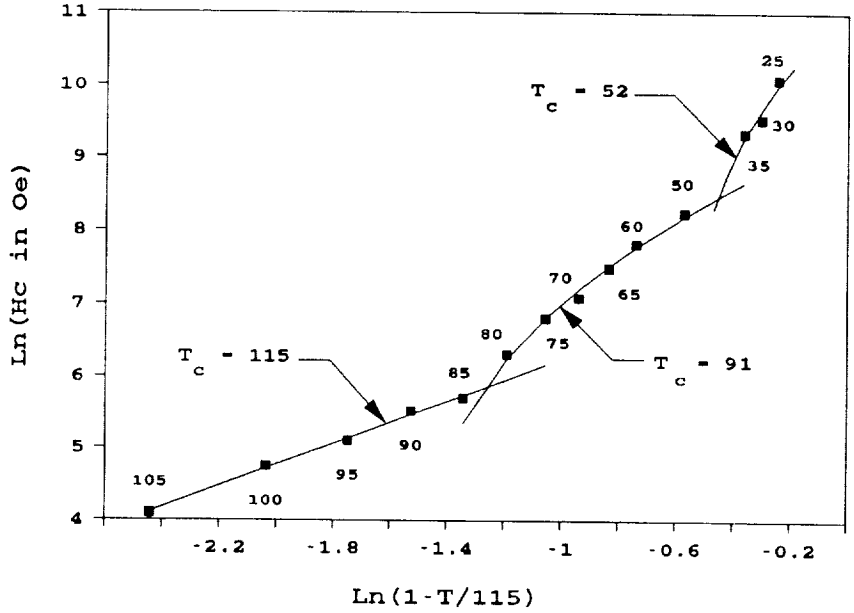

Figure 12. Log-log graph of critical field for flux depinning versus reduced temperature. The three solid lines are linear (see text) least square fits to the data points in their range.

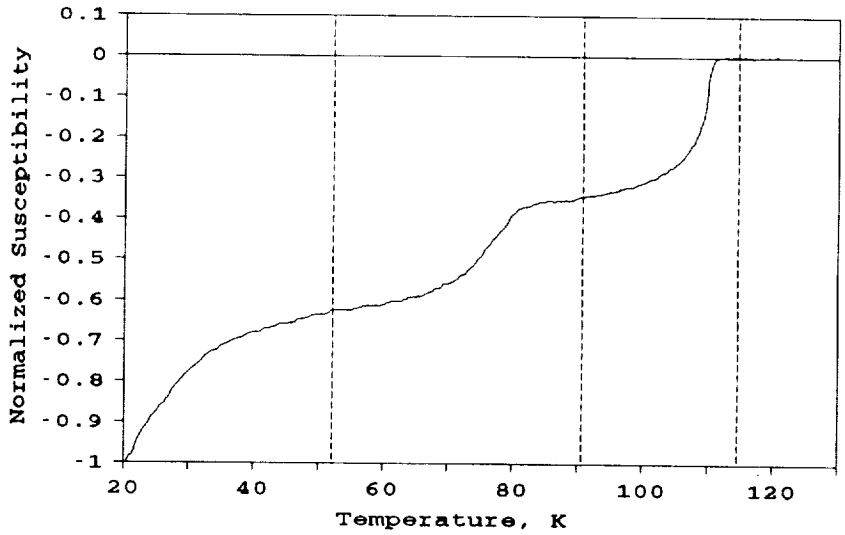

Figure 13. Real part of the ac magnetic susceptibility of the present sample. The three vertical lines are obtained as described in the text.

IV. FLUX DYNAMICS IN HIGHLY-PINNED YBCO

One of the important technological requirements of a superconductor is stability of the flux lattice. When the applied magnetic field is changed suddenly, a transient behavior is observed whereby the magnetization which is initially induced in the superconductor decays exponentially. This "flux flow" was observed to occur in YBCO [18] in the first 10 seconds or so, the actual time depending on the pinning, the field and the temperature. Following this dynamic transient diamagnetic effect, the magnetization decays with a ln(t) behavior as predicted by the Anderson-Kim [19,20] thermally activated flux creep model. Theoretical consideration of the thermoactivated movement of vortices which occur upon application of a magnetic field to a zero-field-cooled high-Tc superconducting sample predicts a further stage in the kinetics of magnetization: following the logarithmic decay with time, (after ~10^5s), equilibrium is approached exponentially [29]. (It is possible that there are two different logarithmic decays asssociated with flux creep in grains and grain boundaries. This is now under investigation.)

Studies of the kinetics of the magnetization allows the pinning characteristics to be determined. From the logarithmic stage of the magnetization vs time curve, it is possible to obtain an activation moment, α = kTR/P, where k is the Boltzmann constant, T is the temperature, R is the effective radius of the sample, and P is the log-creep rate (P=dM/dln(t)). Since the magnitude of P also depends linearly on R, α will not depend on the size of the sample and hence is an intensive characteristic of the material. From the exponential stage, it is possible to obtain the equilibrium magnetization, M_o (or induction, B_o), the time of relaxation, τ, and a vortex diffusion coefficient, $D \simeq R^2/\tau$. Knowing these parameters allows an estimation of the activation energy for the thermoactivated vortex, or vortex bundle, movement, U=kT ln $(T \cdot V_o \cdot B_o \cdot \alpha/kT)$, where V_o is the limiting vortex bundle velocity. V_o is close to the sound velocity [30,31].

These two stages were found by measuring the magnetization as a function of time at different temperatures and applied fields for three samples of $YBa_2Cu_3O_7$ prepared by different processes including a single crystal, a sintered powder, and one prepared by the quench, melt and growth (QMG) method [29,32]. All three samples displayed the same superconducting onset temperature, T_c=93K.

The first sample was a bar 0.9x0.9x5.1 mm^3, with the c direction generally in the plane perpendicular to its long axis, cut from a single grain of a polycrystal produced by the QMG process by K. Sawano of the Nippon Steel Co. The sample can be considered as a bulk superconductor without weak links [32]. The second sample was a bar 2.3xl.7x5.8 mm^3 produced by solid state sintering by J. Blendell of NIST. The sample had a uniform grain structure with a grain size less than 5 μm. The third sample was a single crystal plate 0.9x0.8x0.06 mm^3 prepared at NIST.

Of the three samples studied, only the QMG sample allowed a determination of the effective radius, R, and thus a quantitative estimation of the pinning parameters: activation moment, α, vortex diffusion coefficient, D, and activation energy, U. For a more detailed discussion, see [30]. For the sintered sample, the weak links associated with the grain boundaries causes the effective radius to be a function of magnetic field [33]. The effective radius associated with the single crystal is undetermined because only a portion of it was superconducting.

The samples were cooled to the measuring temperature in zero magnetic field. The magnetic field was then applied and the magnetization, M(t), measured as a function of time

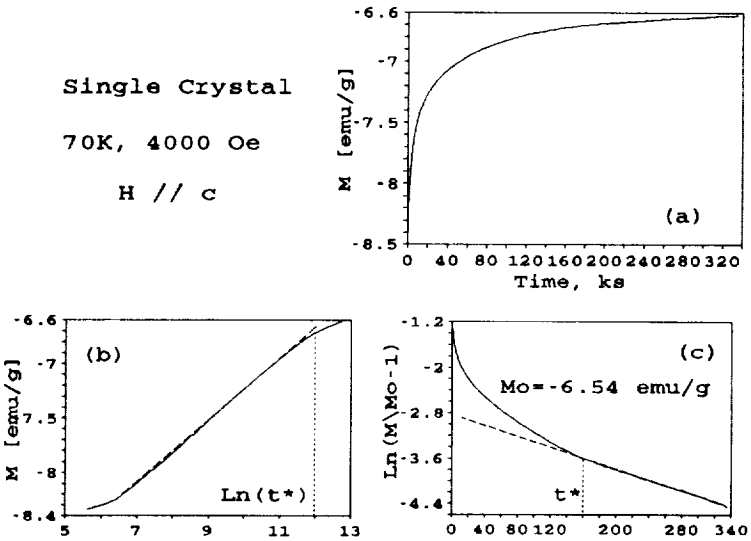

Figure 14. (a) Magnetization, M, vs time, (b) M vs logarithm of time, and (c) logarithm of (M/Mo-1) vs time. The time t* marks the beginning of the approach-to-equilibrium stage. The dashed lines are linear best fits.

using a vibrating sample magnetometer (VSM) for the shorter times, and a commercial SQUID magnetometer for longer times. To approach the equilibrium magnetization, high temperatures (70 and 80K) and long-times (about four days) were necessary. The magnetic fields were applied parallel to the long axis of the bar samples, and perpendicular to the single crystal plate. Magnetization vs time data for the single crystal at 70K and 4kOe, for the sintered sample at 80K and 2kOe, and for the QMG sample at 80K and 2kOe are plotted in Figures 14a, 15a and 16a, respectively. Curves obtained for other temperatures and applied magnetic fields have approximately the same shape as in these Figures: for all the curves there are log-time dependencies in M(t), and for much longer times ($t > t^*$), there are exponential approaches to the equilibrium magnetization, M_0. The magnetization vs logarithm of time curves are displayed in Figures 14b, 15b, and 16b. It is seen, that after about 700 seconds, there are two stages of M(t): (i) a log-time dependence, and (ii) at longer times (after t*) a deviation from the log-time dependence during which the approach to the value of the equilibrium magnetization is obtained [29]. In this time regime, the magnetization, M(t), as illustrated by Figures 14c, 15c, and 16c, obeys an exponential law $M(t) = M_0 + M'\exp(-t/\tau)$, (or $\ln[M/Mo-1] \propto -t/\tau$), where M' is a constant and τ is the relaxation time, for all the samples. The values of the relaxation time, τ, are obtained as the slope of the linear portion of the curves in (c).

Measurements in the logarithmic stage give the log-creep rate, P. The temperature dependences of P are plotted at a number of magnetic fields for the QMG and the sintered sample in Figure 17. These curves are similar to those shown earlier in conventional [34] and high-temperature single crystal [23] and

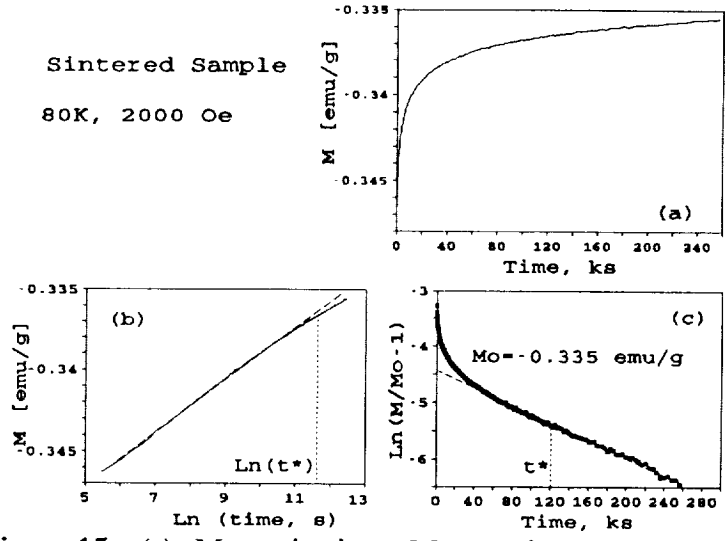

Figure 15. (a) Magnetization, M, vs time, (b) M vs logarithm of time, and (c) logarithm of (M/Mo-1) vs time. The time t* marks the beginning of the approach-to-equilibrium stage. The dashed lines are linear best fits.

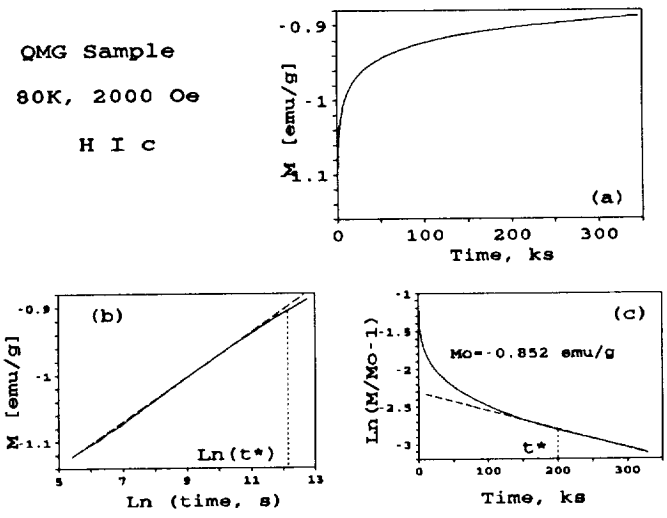

Figure 16. (a) Magnetization, M, vs Time, (b) M vs logarithm of time, and (c) logarithm of (M/Mo-1) vs time. The time t* marks the beginning of the approach-to-equilibrium stage. The dashed lines are linear best fits.

thin film [35] superconductors. For the QMG sample with its effective radius, $R \approx 0.045$ cm, α can be derived. Values of the activation moment α, normalized to ϕ_0 (the magnetic flux of one vortex $=2.07\text{x}10^{-7}$ Gcm^2) are plotted in Figure 18. It is seen that, for large enough fields (2 and 4 kOe), α is almost independent of temperature for temperatures below where the maximum in P occurs. Taking into account that $\alpha/\phi_0 = n \cdot \ell 1 \cdot \ell 2$, where n is the number of vortices in a bundle, $\ell 1$ is the displacement of the vortex or bundle at an activation event, and $\ell 2$ is the effective length of a displaced section of the bundle, it is possible to estimate the parameters of an activation event. For the QMG sample at 4kOe, for example, assuming that $n \simeq 1$, we can conclude that $\ell 1 \simeq \ell 2 \simeq 3\text{x}10^{-6}$cm. The growth of α at higher temperatures is likely due to the increase in the number of vortices in the bundle.

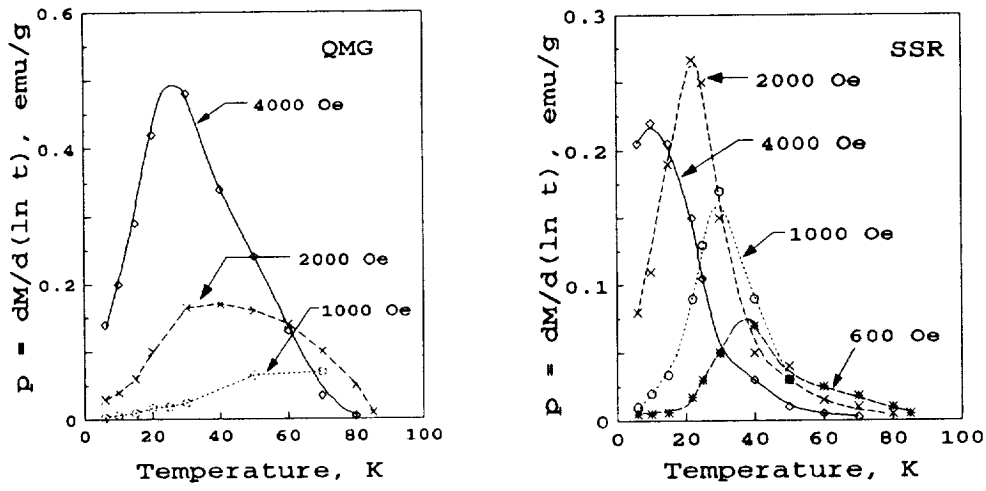

Figure 17. Log-creep rate, P, for the QMG (quench and melt growth) and sintered YBCO samples.

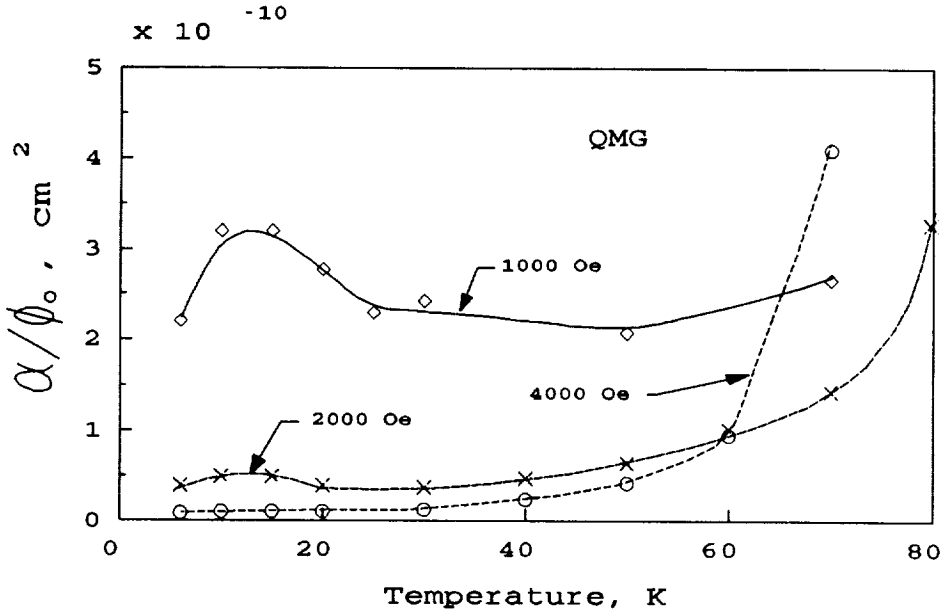

Figure 18. Temperature dependence of α/ϕ_0 at a number of magnetic fields for the QMG sample.

V. SUMMARY

There is still much to be learned concerning the flux flow and flux dynamics in high-temperature superconductors. We have described herein some recent studies on YBCO single crystals which show that twin planes have a small, but measureable, effect on flux pinning. Single crystals with a high degree of perfection appear to have considerably reduced pinning at higher temperatures.

In samples of Bi-Sr-Ca-Cu, we found that there was a critical field for flux depinning which was sample dependent and which could be described by a power law in the reduced temperature using an exponent of 1.5.

Samples of $YBa_2Cu_3O_{6+x}$ prepared by three different techniques were found to display a universal magnetization vs time behavior: after an initial transient at small enough times there is a log-time stage. At much longer times, M(t) approaches equilibrium exponentially [29]. The log-rate of magnetization P=dM/dln(t), can be used to determine the "activation moment", if the effective radius of a sample is known [29]. By analysis of kinetics of both the log-stage and the approach to equilibrium it is possible to determine an activation energy for the vortex movement. Details are given in [30,31].

VI. ACKNOWLEDGEMENTS

The various results described in this paper were carried out in close cooperation with many colleagues and coworkers from NIST and elsewhere. We want to especially acknowledge the following people from National Institute of Standards and Technology - R.D. Shull, D. Lundy, C.K. Chiang, F. Gayle, J.E. Blendell, J. Ritter, J.S. Wallace, W. Wong-Ng, R.S. Roth, L.P. Cook, A.J. Shapiro, R. Brown, R. Drew, D. Mathews, T. Chen, E. Keisman, and M. Hill; from The Johns Hopkins University/Applied Physics Lab - K. Moorjani, J. Bohandy, B.F. Kim, F.J. Adrian, T.E. Phillips, W.J. Green, and E. Agostinelli; from the Naval Research Laboratory - M. Rubinstein; from the Nippon Steel Corporation - K. Sawano; from the Israel Nuclear Center - U. Atzmony, M. Melamed, and H. Ettedgui, and from Superconix, Inc - C.F. Gallo

REFERENCES

1. A.A. Abrikosov, Soviet Physics JETP, 5, 1442 (1957).

2. D.L. Kaiser, F. Holtzberg, B.A. Scott, and T.R. McGuire, Appl. Phys. Lett., 51, 1040 (1987); D.L. Kaiser, F. Holtzberg, M.F. Chisholm, and T.K. Worthington, J. Cryst. Growth 85, 593 (1987).

3. T.R. Dinger, T.K. Worthington, W.J. Gallagher, and R.L. Sandstrom, Phys Rev. Lett. 58, 2687 (1987).

4. G.W. Crabtree, J.Z. Liu, A. Umezawa, W.K. Kwok, C.H. Sowers, S.K. Malik, B.W. Veal, D.J. Lam, M.B. Brodsky, and J.W. Downey, Phys. Rev. B, 36, 4021 (1987).

5. W.J. Gallagher, J. Appl. Phys., 63, 4216 (1988).

6. T.W. Worthington, Y. Yeshurun, A.P. Malozemoff, R.M. Yandrofski, F.H. Holtzberg, and T.R. Dinger, J. de Phys. 49, C8-2093 (1988).

7. T.K. Worthington, W.J. Gallagher, D.L. Kaiser, F.H. Holtzberg, and T.R. Dinger, Physica C, 153-155, 32 (1988).

8. L. Fruchter, M. Oussena, C. Giovannella, and I.A. Campbell, Supercond. Sci. Technol., 1, 75 (1988).

9. L.J. Swartzendruber, A. Roitburd, D.L. Kaiser, F.W. Gayle, and L.H. Bennett, Phys. Rev. Lett. 64, 483 (1990).

10. P.H. Kes, Physica C 153-155, 1121 (1988).

11. L.Ya. Vinnikov, L.A. Gurevich, G.A. Yemelchenko, and Yu.A. Ossipyan, Solid State Comm., 67, 421 (1988).

12. G.J. Dolan, G.V. Chandrashekhar, T.R. Dinger, C. Feild, and F. Holtzberg, Phys. Rev. Lett., 62, 827 (1989).

13. E.M. Gyorgy, R.B. van Dover, K.A. Jackson, L.F. Schneemeyer, and J.V. Waszczak, Appl. Phys. Lett. 55, 283 (1989).

14. A. Roitburd, L.J. Swartzendruber, D.L. Kaiser, F.W. Gayle, and L.H. Bennett, Phys. Rev. Lett. 64, 2962 (1990).

15. D. Kaiser, these proceedings.

16. H. Maeda, Y. Tanaka, M. Fukutomi, and T. Asano, Jap. J. Appl. Phys. Lett. 27, L209 (1988).

17. C. W. Chu, L. Bechtold, L. Gao, P. H. Hor, Z. J. Huang, et al., Phys. Rev. Lett. 60, 941 (1988).

18. U.Atzmony, R.D. Shull, C.K. Chiang, L.J. Swartzendruber, L.H. Bennett, and R.E. Watson, J. Appl. Phys. 63, 4179 (1988).

19. P.W. Anderson, Phys. Rev. Lett. 9, 309 (1964).

20. Y.B. Kim, C.F. Hempstead, and A.R. Strnad, Phys. Rev. Lett. 12, 145 (1964).

21. K.A. Müller, M. Takashige, and J.G. Bednorz, Phys. Rev. Lett. 58, 1143 (1987).

22. I. Morgenstern, K.A. Müller, and J.G. Bednorz, Z. Phys. B 69, 33 (1987).

23. Y. Yeshurun and A.P. Malozemoff, Phys. Rev. Lett. 60, 2202 (1988).

24. P.L. Gammel, L.F. Schneemeyer, J. V. Waszczak, and D. J. Bishop, Phys. Rev. Lett. 61, 1666 (1988).

25. T.T.M. Palstra, B. Batlogg, L.F. Schneemeyer, and J.V. Waszczak, Phys. Rev Lett. 61, 1662 (1988).

26. L.J. Swartzendruber, L.H. Bennett, and C.F. Gallo, in "Proceedings of High-T_c Superconductors: Magnetic Interactions" edited by L.H. Bennett, Y. Flom, and G.C. Vezzoli (World Scientific Publishing Co., New Jersey, 1989). p.303

27. D.R. Lundy, J. Ritter, L.J. Swartzendruber, R.D. Shull, and L.H. Bennett, in "Proceedings of High-T_c Superconductors: Magnetic Interactions" edited by L.H. Bennett, Y. Flom, and G.C. Vezzoli (World Scientific Publishing Co., New Jersey, 1989). p.263

28. F.J. Adrian, J. Bohandy, B.F. Kim, K. Moorjani, J.S. Wallace, R.D. Shull, J.J.

Swartzendruber, and L. H. Bennett, Physica C 156, 184 (1988).

29. M. Turchinskaya, L.H. Bennett, L.J. Swartzendruber, A. Roitburd, C.K. Chiang, M. Hill, J.E. Blendell, and K. Sawano, in "High-Temperature Superconductors: Fundamental Properties and Novel Materials Processing" Mat. Res. Soc. Symp. Proc. 169, 957 (1990).

30. A.L. Roitburd, and M.T. Turchinskaya, these proceedings.

31. A.L. Roitburd, M.T. Turchinskaya, L.H. Bennett, and L.J. Swartzendruber, "Vortex Diffusion Coefficient in YBaCuO", Phys. Rev. Lett. in press (1990).

32. M. Murakami, M. Morita, and N. Koyama, Jpn. J. Appl. Phys., 28, L1125 (1989).

33. J.W. Ekin, T.M. Larson, A.M. Herman, Z.Z. Sheng, K. Togano, and H. Kumakura, Physica C (in press).

34. M.R. Beasley, R. Labush, and W.W. Webb, Phys. Rev. 181, 682 (1969).

35. C. Rossel and P. Chaudhari, Physica C, 153-155, 306 (1988).